Carbohydrate Polymers 100 (2014) 24–30

Contents lists available at ScienceDirect

Carbohydrate Polymers

journal homepage: www.elsevier.com/locate/carbpol

Ice templated and cross-linked xylan/nanocrystalline cellulose hydrogels

Tobias Köhnke[a,b], Thomas Elder[c], Hans Theliander[b], Arthur J. Ragauskas[a,*]

[a] Institute of Paper Science and Technology, Georgia Institute of Technology, Atlanta, GA 30332, USA
[b] Forest Products and Chemical Engineering, Department of Chemical and Biological Engineering, Chalmers University of Technology, SE-412 96 Gothenburg, Sweden
[c] USDA-Forest Service, Southern Research Station, 2500 Shreveport Highway, Pineville, LA 71360, USA

ARTICLE INFO

Article history:
Received 4 June 2012
Received in revised form
13 December 2012
Accepted 3 March 2013
Available online 26 March 2013

Keywords:
Cellulose nanocrystals
Cellulose whiskers
Freeze-casting
Hydrogel
Xylan

ABSTRACT

Structured xylan-based hydrogels, reinforced with cellulose nanocrystals (CNCs), have successfully been prepared from water suspensions by cross-linking during freeze-casting. In order to induce cross-linking during the solidification/sublimation operation, xylan was first oxidized using sodium periodate to introduce dialdehydes. The oxidized xylan was then mixed with CNCs after which the suspension was frozen unidirectionally in order to control the ice crystal formation and by that the pore morphology of the material. Finally the ice crystal templates were removed by freeze-drying. During the freeze-casting process hemiacetal bonds are formed between the aldehyde groups and hydroxyl groups, either on other xylan molecules or on CNCs, which cross-links the system. The proposed cross-linking reaction was confirmed by using cross-polarization magic angle spinning (CP/MAS) nuclear magnetic resonance (NMR) spectroscopy. The pore morphology of the obtained materials was analyzed by scanning electron microscopy (SEM). The materials were also tested for compressive strength properties, both in dry and water swollen state. All together this study describes a novel combined freeze-casting/cross-linking process which enables fabrication of nanoreinforced biopolymer-based hydrogels with controlled porosity and 3-D architecture.

1. Introduction

Hydrogels are physically and/or chemically cross-linked polymer networks that are able to absorb large amounts of water. There are numerous applications for hydrogels, especially in the medical and pharmaceutical industry due to their excellent biocompatibility, soft tissue consistency resemblance and permeability to metabolites and oxygen (Peppas, Bures, Leobandung, & Ichikawa, 2000; Peppas, Hilt, Khademhosseini, & Langer, 2006). Along with a wide range of synthetic polymers, various biopolymers have been investigated for hydrogel formulations, typically hyaluronic acid, chitosan, cellulose and starch derivatives, alginate, dextran, collagen, and gelatin (Van Vlierberghe, Dubruel, & Schacht, 2011). Polysaccharides have a number of advantages over synthetic polymers as hydrogel components since they usually are abundant, renewable, biocompatible, biodegradable, non-toxic, and may have unique properties that cannot be easily mimicked through chemical synthesis (Coviello, Matricardi, Marianecci, & Alhaique, 2007). In the current trend for a more effective utilization of biomass (Ragauskas et al., 2006), hemicelluloses have emerged as a new potential group of polysaccharides in the development of new materials. Even though hemicelluloses, such as xylans, mannans and xyloglucans, are known to have gelling and film forming properties appropriate for production of biodegradable hydrogels (cf. Ebringerová, Hromádková, Heinze, 2005), relatively few examples of hemicelluloses-based hydrogels have been reported in the literature (Lindblad, Sjöberg, Albertsson, & Hartman, 2007). However, during the last couple of years the emerging interest in research on advanced materials based on renewable biopolymer resources have resulted in a number of publications which clearly demonstrates the potential of using xylan in hydrogel formulations (e.g. Chimphango, van Zyl, & Görgens, 2012; Karaaslan, Tshabalala, Yelle, & Buschle-Diller, 2011; Meena, Lehnen, Schmitt, & Saake, 2011; Peng, Ren, Zhong, Peng, & Sun, 2011; Pohjanlehto, Setälä, Kammiovirta, & Harlin, 2011; Silva, Habibi, Colodette, & Lucia, 2011).

Xylans are the most common hemicelluloses, and constitute 25–35% of the dry biomass of woody tissues of dicots and lignified tissues of monocots and occur up to 50% in some tissues of cereal grains (Ebringerová & Heinze, 2000). In terrestrial plants, xylans are heteropolymers, possessing a linear

---

* Corresponding author. Tel.: +1 404 894 9701; fax: +1 404 894 4778.
E-mail addresses: art.ragauskas@ipst.gatech.edu, arthur.ragauskas@ipst.gatech.edu (A.J. Ragauskas).

0144-8617/$ – see front matter © 2013 Elsevier Ltd. All rights reserved.
http://dx.doi.org/10.1016/j.carbpol.2013.03.060

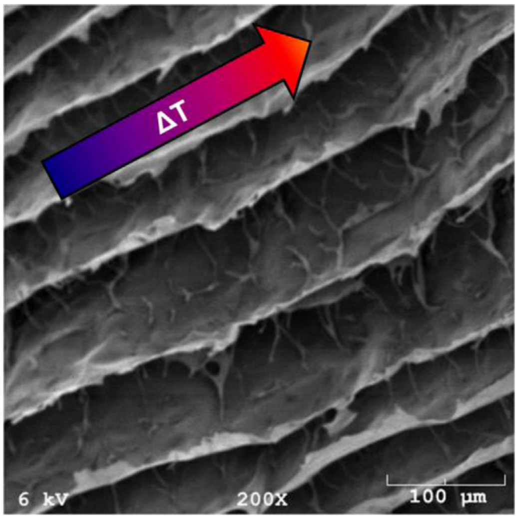

Fig. 1. SEM image of a freeze-cast xylan–cellulose nanocrystal composite foam cross-section. The lamellar structure is aligned with the temperature gradient imposed during the solidification process.

β-(1→4)-D-xylopyranan backbone substituted with a number of different side chains/groups, where L-arabinofuranosyl and 4-*O*-methyl-D-glucopyranosyl uronic acid units are most common. The great abundance of xylan in nature, along with the fact that xylans are readily available in residues and side-streams in the forestry/pulp and agricultural industry, makes xylans highly attractive as biopolymer resources in the development of new green materials (Hansen & Plackett, 2008). Furthermore, the xylan backbone has an affinity to cellulose and will adsorb irreversibly on cellulosic surfaces, a propensity that provides great opportunities for the use of xylans in cellulose-based composites (Köhnke, Brelid, & Westman, 2009; Köhnke, Lund, Brelid, & Westman, 2010; Köhnke, Östlund, & Brelid, 2011).

We have recently reported that highly structured biofoams can be prepared from xylan and cellulose nanocrystal (CNC) suspensions by employing an ice-templating technique (Köhnke, Lin, Elder, Theliander, & Ragauskas, 2012; Köhnke, Theliander, & Ragauskas, 2012). The ice-templating technique, also known as freeze-casting, involves freezing of an aqueous suspension followed by sublimation of the solidified phase under reduced pressure (cf. Deville, 2008; Gutiérrez, Ferrer, & del Monte, 2008; Wegst, Schecter, Donius, & Hunger, 2010). During the freezing operation, xylan molecules and CNCs are rejected from the moving solidification front, concentrated and finally entrapped between the growing solvent crystals. Consequently, this ice-segregation-induced self-assembly process yields materials with porous structures where the pores are a replica of the ice crystals. By employing unidirectional solidification we were able to design low density xylan biofoams which possessed a lamellar structure (Fig. 1), a porosity of 92–95% and a very high degree of pore interconnectivity (>99%) (Köhnke, Lin, et al., 2012; Köhnke, Theliander, et al., 2012).

If these biofoams could be stabilized by cross-linking, the applied freeze-casting process would enable fabrication of polysaccharide based hydrogels with controlled porosity and 3-D architecture. It is widely accepted that aldehyde groups in polysaccharides react with nearby hydroxyl groups to form intra- and inter-chain hemiacetals (cf. Kristiansen, Potthast, & Christensen, 2010). The formation of these bonds is known to influence oxidation reactions (Painter & Larsen, 1970), induce aggregation (Maia, Carvalho, Coelho, Simões, & Gil, 2011) or even gelation (Christensen, Aasprong, & Stokke, 2001). It has recently been reported that micro fibrillated cellulose containing aldehyde groups may form hemiacetal bonds during freeze-drying (Brodin & Theliander, 2012), which increases the water wet integrity of the material in analogy with aldehyde containing wet-strength resins in papermaking (cf. Chen, Hu, & Pelton, 2002; Saito & Isogai, 2006). In this study we want to investigate if this cross-linking approach could be used to stabilize our freeze-cast nanoreinforced xylan-based biofoams and by that increase the wet integrity of the material. An important consequence of unidirectional solidification is the ice-segregation-induced self-assembly. This will concentrate the oxidized xylan polymers, bringing the molecules into closer contact, which would promote the formation of cross-linking hemiacetal bonds.

The investigated procedure to form xylan–cellulose nanocrystal composite hydrogels, including the proposed cross-linking mechanism, is presented in Fig. 2. Xylan is first oxidized using sodium periodate to introduce dialdehydes. The oxidized xylan is then mixed with CNCs, frozen and freeze-dried. During the freeze-casting process hemiacetal bonds are formed between the aldehyde groups and hydroxyl groups, either on other xylan molecules or on CNCs, which cross-links the system. This combined freeze-casting/cross-linking process would enable the fabrication of polysaccharide based hydrogels with controlled porosity and 3-D architecture.

2. Experimental

2.1. Material

Oat spelt glucuronoarabinoxylan (GAX) was obtained from Sigma–Aldrich. This xylan fraction has been reported to contain 81% xylose, 9.8% arabinose, 7.6% glucose, 1.4% galactose and 0.2% of mannose (Saxena & Ragauskas, 2009).

2.2. Oxidation of xylan

Introduction of aldehyde groups to xylan was performed by oxidation using sodium periodate. A solution of GAX was prepared by heating a mixture of 5.00 g GAX and 100 mL deionized water to boiling under stirring. The solution was then cooled to room temperature, after which a specific amount of $NaIO_4$ (1.00, 3.00, 5.00 mmol/g GAX), dissolved in 100 mL deionized water, was added. The solution was stirred for 24 h in the absence of light at room temperature. The product was then purified by dialysis (Spectra Por 2, MWCO: 12–14 kDa) against deionized water. One part of the oxidized GAX was reduced with sodium borohydride. The pH of 40 mL oxidized dialyzed xylan solution was increased to 8 by addition of a few drops of 0.1 M NaOH, after which 0.5 g $NaBH_4$ was

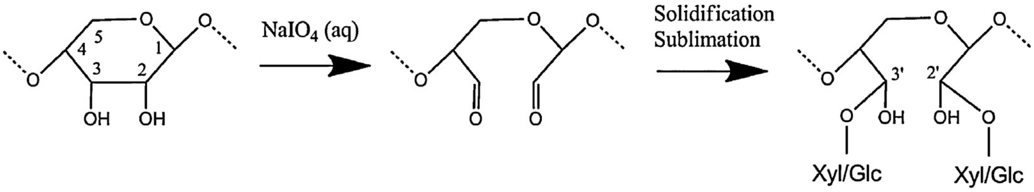

Fig. 2. Proposed reactions involved in cross-linking of xylan–cellulose nanocrystal composite hydrogels during freeze-casting.

added. The solution was stirred for 24 h in the absence of light at room temperature. The pH of the solution was then decreased to 6 by adding glacial acetic acid. The product was purified by dialysis (Spectra Por 2, MWCO: 12–154 kDa) against deionized water.

To estimate the degree of oxidation a method similar to that described by Zhao and Heindel (1991) was used, where added hydroxylamine hydrochloride reacts quantitatively with all available carbonyls while releasing protons. Briefly, 0.100 g xylan was suspended in 25 mL of a 0.25 M hydroxylamine hydrochloride solution adjusted to pH 4.0 with NaOH. After 2 h under stirring at room temperature the suspension was titrated back to 4.0 with 0.100 N NaOH. The degree of oxidation was calculated from the amount of NaOH required. Three replicates per sample were analyzed.

2.3. *CP/MAS NMR spectroscopy*

The NMR samples were prepared by loading the samples into 4 mm cylindrical ceramic MAS rotors. Repetitive steps of packing the sample into the rotor were done to fully compress and load the maximum amount of sample. ^{13}C CP/MAS solid-state NMR measurements were carried out on dry samples in a Bruker DSX-400 spectrometer operating at a frequency of 100.55 MHz for ^{13}C NMR in a Bruker double-resonance MAS probe head at a spinning speed of 10 kHz. CP/MAS experiments utilized a 5 μs (90°) proton pulse, 1.5 ms contact pulse, 4 s recycle delay and 2 K scans. ^{1}H MAS solid-state NMR experiments were carried out on samples swollen in 100% D_2O for 48 h and performed on a Bruker DSX-400 spectrometer, operating at a frequency of 399.875 MHz for ^{1}H NMR in a Bruker double-resonance MAS probe head at spinning speed of 2 kHz. A standard one pulse sequence utilized a 5 μs (90°) proton pulse, 10 s recycle delay and 128 scans.

2.4. *Preparation of cellulose nanocrystals*

Cellulose nanocrystals (CNCs) were prepared by sulfuric acid hydrolysis of microcrystalline cellulose (Avicel PH-101 from Sigma–Aldrich). In brief, 68.00 g (dry weight) microcrystalline cellulose was mixed with 600 mL of a preheated (45 °C) 64% (w/w) aqueous H_2SO_4 solution under continuous stirring for 130 min. The hydrolysis reaction was stopped by adding an excess of deionized water followed by the removal of acidic solution by successive centrifugation until the supernatant became turbid. The sediment was collected and dialyzed (Spectra Por 2; MWCO: 12–14 kDa) until the pH of the solution became neutral. The content was sonicated (using a Model CU33 tapered ultrasonic cell disruptor horn from PGC Scientific, bearing a 12.7 mm tip and controlled with a GEX 500 ultrasonic processor, Sonics & Materials, with an output amplitude of 40%) in an ice bath for 6 min and centrifuged. The turbid supernatant, containing CNCs, was collected and the remaining sediment was again mixed with deionized water, sonicated and centrifuged to obtain additional CNCs; a procedure that was repeated until the supernatant was clear. CNCs were obtained in 50% yield. Atomic force microscopy (AFM) analysis of the obtained CNCs (Fig. 3a) revealed individual CNCs which possessed average width (i.e. height) of 11 ± 2 nm and length in the range of several hundreds of nanometers. The CNCs suspension also showed birefringence (Fig. 3b), which provided supporting evidence for the existence of rod-like CNCs (Eichhorn, 2011).

2.5. *Freeze-casting*

Xylan solutions were prepared by heating mixtures of xylan and deionized water to boiling under stirring. Suspensions for the xylan–CNC composite foams were prepared by mixing an equal volume of a 1.25% (w/w) CNC suspension and a 5% (w/w) xylan solution at room temperature. A solution/suspension volume of 1.00 mL was transferred into glass ampoules, which were immersed in liquid nitrogen for 5 min. In order to ensure unidirectional freezing, only the bottom of the ampoule was in contact with liquid nitrogen and vertical heat transfer was prevented by insulation of the ampoule using polystyrene foam. Frozen samples were immediately put in a freeze-dryer to remove ice crystal templates by sublimation. The average diameter of the cylindrical samples after freeze-drying was 10 mm.

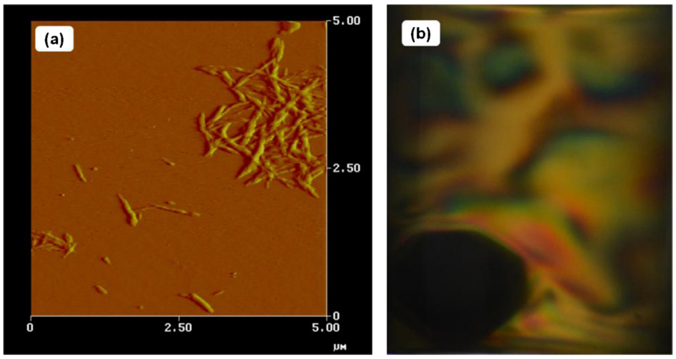

Fig. 3. (a) AFM image of obtained cellulose nanocrystals (CNCs). (b) Shear-induced birefringence of a 1% (w/w) CNC suspension viewed between crossed polars.

2.6. *Scanning electron microscopy*

Prior to structural analysis the cylindrical samples were pulled into two pieces using two forceps. The pore morphology of the exposed inner surface parallel to the cylinder axis was studied after imaging of gold coated samples using a Hitachi S-800 Field Emission Gun (FEG) Scanning Electron Microscope (SEM) operated at 6 kV.

2.7. *Mechanical testing*

Compressive tests were carried out on a Bose ELF 3200 using load cells of 4.9 N or 24.9 N. Due to a small surface roughness a preload of approximately 0.05 N was applied to the cylindrical foam samples before initiating compression testing in the direction parallel to the cylinder axis. The compression rate of the crosshead was set to 0.1 mm/s. The modulus was calculated from the initial linear region (strain < 5%) of the stress–strain curves. Most materials showed a gradual transition from linear to non-linear stress–strain behavior with no pronounced horizontal plateau region, which consequently made it difficult to assign the yield point. Therefore, the materials were additionally compared by the stress at 50% strain. The dry samples were stored in a desiccator until analysis. The hydrogels were soaked in deionized water for 30 min before testing. Mechanical compression data were averaged over six specimens.

3. Results and discussion

3.1. *Cross-linking during freeze-casting*

To investigate if hemiacetal bonds can be formed in aldehyde xylan during freeze-casting and by that cross-link ice-templated hydrogels, oat spelt glucuronoarabinoxylan (GAX) was oxidized to different degrees with $NaIO_4$ (Table 1), freeze-dried and analyzed using cross-polarization magic angle spinning (CP/MAS) nuclear magnetic resonance (NMR) spectroscopy.

^{13}C CP/MAS NMR spectra for the reference xylan (GAX) and oxidized xylans (GAX ox), as well as for a xylan sample first oxidized and then reduced by $NaBH_4$ (GAX ox-5-red), are shown in

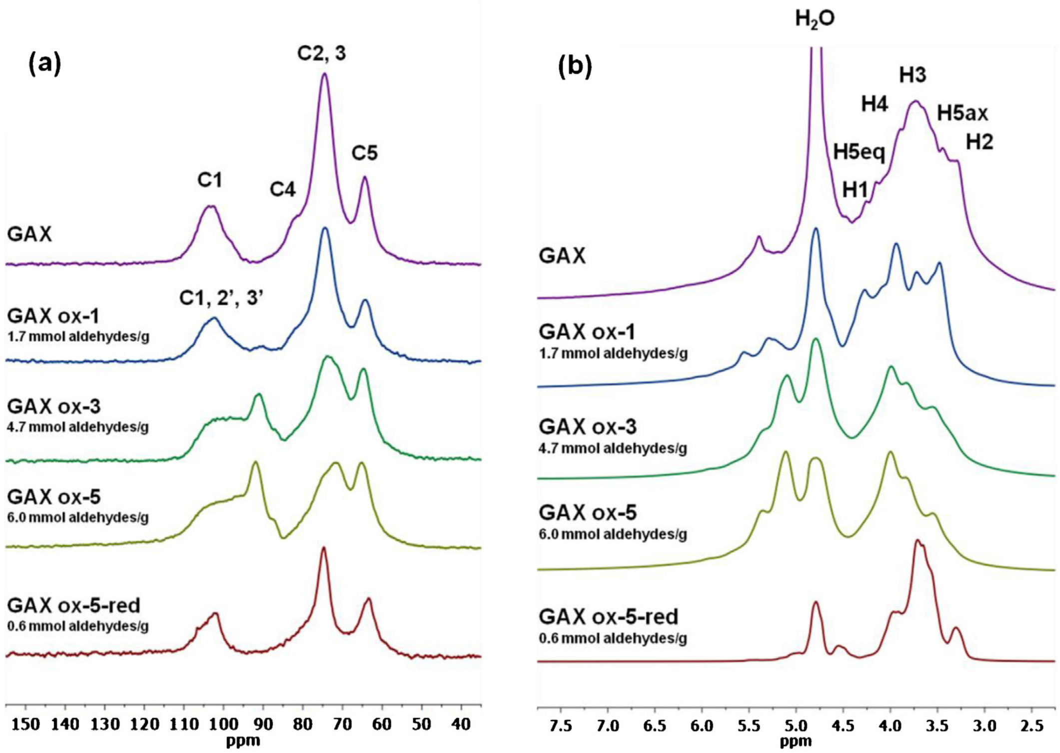

Fig. 4. ^{13}C (a) and ^{1}H (b) CP/MAS NMR spectra for freeze-dried reference xylan (GAX), oxidized xylans (GAX ox), and for a xylan sample first oxidized and then reduced by $NaBH_4$ (GAX ox-5-red). Cf. Fig. 2 for carbon numbering.

Fig. 4a. A characteristic feature of the oxidized samples is the lack of carbonyl signal expected around 200 ppm, even at high oxidation degrees. This is a first indication that the aldehyde groups are forming hemiacetals with remaining xylan hydroxyl groups during the solidification/sublimation process. It is also evident that $NaIO_4$ oxidation reduces signals from C2 and C3 around 75 ppm, while new signals appear in the spectral region of 125–85 ppm, most probably from C2 and C3 involved in hemiacetal bonds (denoted C2′ and C3′). This statement is in line with what can be seen in the spectrum of the reduced sample (GAX ox-5-red). ^{1}H CP/MAS NMR spectra of the same samples are shown in Fig. 4b. It is clear that the relative peak intensities for H2 and H3 (~3.8–3 ppm) are reduced due to the oxidation, as expected, and that new signals appear in the anomeric region (6–4.5 ppm). This, along with the fact that no carbonyl signal was seen around 9.5 ppm, strengthens the conclusions drawn from the ^{13}C analyses that hemiacetal bonds are formed in aldehyde xylan during freeze-casting.

The application of ^{13}C CP/MAS NMR spectroscopy for nondestructive analysis of material difficult to dissolve or the analysis of material ultrastructure was acknowledged at its inception (Schaefer & Stejskal, 1976). This type of solid-state NMR is well-suited for the analysis of complex polymer systems and has been applied to isolated plant biopolymers and intact plant tissue for decades. However, ^{13}C CPMAS NMR produces broad resonance lines and in plant biopolymers are typically results in complex spectra of overlapping signatures. This along with variations in relaxation time, chemical shift anisotropy, cross-polarization efficiency and field homogeneity make a single ^{13}C CPMAS NMR at best semi-quantitative (Aliev & Law, 2003; Duer, 2002). Though true, with a properly chosen recycle delay and cross-polarization time these effects can be minimized. Several approaches have been effectively applied to account for the spectral interference of overlapping signature displayed in most plant biopolymers also demonstrating the power of relative comparison to detect changes between sample or upon treatment and near quantitative validity of ^{13}C CP/MAS NMR (Leary, Morgan, Newman, Samuelsson, & Westermark, 1986; Newman & Hemmingson, 1990; Park, Johnson, Ishizawa, Parilla, & Davis, 2009). Assuming the carbon assignments shown in Fig. 4a, relative peak areas can be determined for all the carbons in the system (Table 2). The relative peak area for C1 in the reference xylan fraction (GAX) was found to be 0.2, which is in excellent agreement of what is expected for pentoses like xylan and demonstrates the validity of the method. As shown in Table 2, the fraction of carbons number 2 and 3 involved in hemiacetal bonding is close to the theoretical maximum. All together, it can be concluded that the majority of the aldehyde groups forms hemiacetal bonds during the freeze-casting process and the higher the degree of oxidation the higher the degree of cross-linking.

Since xylan/CNCs are soluble/dispersible in water there is a simpler but still evident way to illustrate that samples containing oxidized xylan are cross-linked upon freeze-casting; and that is to just immerse the materials in water. In Fig. 5a it can clearly be seen that freeze-cast xylan disperses in contact with water, while freeze-cast oxidized xylan does not. The cylindrical sample shape formed during the freeze-casting process is, however, destroyed upon swelling. Interestingly, if the same experiment is performed with freeze-cast xylan foams that contain 20% (w/w) CNCs, the

Table 1
Degree of glucuronoarabinoxylan (GAX) oxidation.

Sample	Added $NaIO_4$ (mmol/g GAX)	Aldehyde groups[a] (mmol/g GAX)	Yield (%)
GAX	0.0	0.0	–
GAX ox-1	1.0	1.7	85
GAX ox-3	3.0	4.7	75
GAX ox-5	5.0	6.0	60

[a] Determined using a hydroxylamine hydrochloride titration method.

Table 2
Relative peak areas from ^{13}C CP/MAS NMR analyses of the reference (GAX) and oxidized xylans (GAX ox).

Sample	Relative peak area		$C2' + C3'$[c]	$C2 + C3$	$C2' + C3'/C2' + C3' + C2 + C3$	Theoretical maximum[d]
	125–85 ppm[a]	85–50 ppm[b]				
GAX	0.20	0.80	0.00	0.40	0.00	0.00
GAX ox-1	0.26	0.74	0.06	0.34	0.16	0.13
GAX ox-3	0.35	0.65	0.15	0.25	0.39	0.40
GAX ox-5	0.48	0.52	0.28	0.12	0.70	0.66

[a] C1, C2′, C3′ region.
[b] C2–5 region.
[c] Assuming relative area of C1 is constant.
[d] Based on added amount of $NaIO_4$.

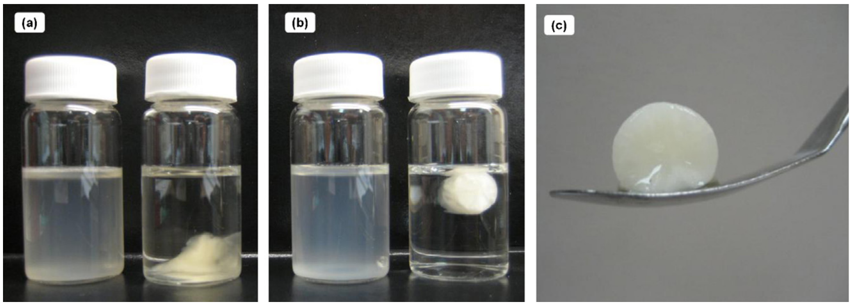

Fig. 5. (a) Freeze-cast xylan foams, containing (left) reference xylan (right) oxidized xylan, immersed in water. (b) Freeze-cast xylan–cellulose nanocrystal composite foams, containing (left) reference xylan (right) oxidized xylan, immersed in water. (c) A xylan–cellulose nanocrystal composite hydrogel containing about 96% (w/w) water.

structure is maintained (Fig. 5b) and free-standing hydrogels are formed with a water holding capacity of about 25 g H_2O/g material (Fig. 5c). These results indicate that cross-linking does occur during the freeze-casting process and that CNC reinforcement of the oxidized xylan gels helps to preserve the structures formed during the freeze-casting process upon swelling in water. To further test the hypothesis that aldehyde xylan forms hemiacetal bonds in polysaccharide matrixes during freeze-casting, the same trials were performed using the reduced oxidized xylan. These foams were easily dispersed in water and did consequently not form gels.

3.2. Pore morphology

The pore morphology of ice-templated foams containing oxidized xylan and CNCs were analyzed by using SEM. As can be seen in Fig. 6a highly ordered porous structure was formed during the freeze-casting process. The formed material is composed of aligned lamellae with a thickness of a couple micrometers separated with a spacing of about 20–50 μm. No significant difference was seen between samples containing xylans possessing different degrees of oxidation. A similar structure was earlier reported for unidirectionally ice-templated foams containing unoxidized xylan and CNCs (Fig. 1; Köhnke, Lin, et al., 2012; Köhnke, Theliander, et al., 2012).

3.3. Mechanical properties

Freeze cast materials containing GAX, oxidized to different degrees (cf. Table 1), and 20% (w/w) CNCs were made and tested for compressive properties. As shown in Fig. 7a and Table 3, the strength properties of the dry biofoams decreased with increased degree of oxidation. At first this might be unexpected since a higher degree of oxidation would lead to a higher cross-linking density of the material. However, this trend is probably due to changes in the rigidity of the xylan polymer chain upon oxidation (cf. Kristiansen et al., 2010), since the reaction involves opening of the xylan pyranose ring (Fig. 2). This is to some extent confirmed by

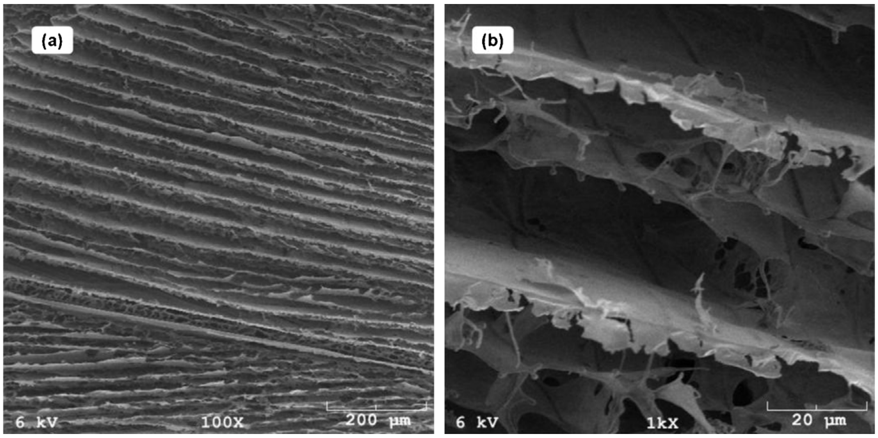

Fig. 6. Cross-section of an ice-templated, unidirectionally solidified, foam containing oxidized xylan (6 mmol aldehydes/g) and cellulose nanocrystals (20%). SEM magnification: (a) 100× (b) 1000×.

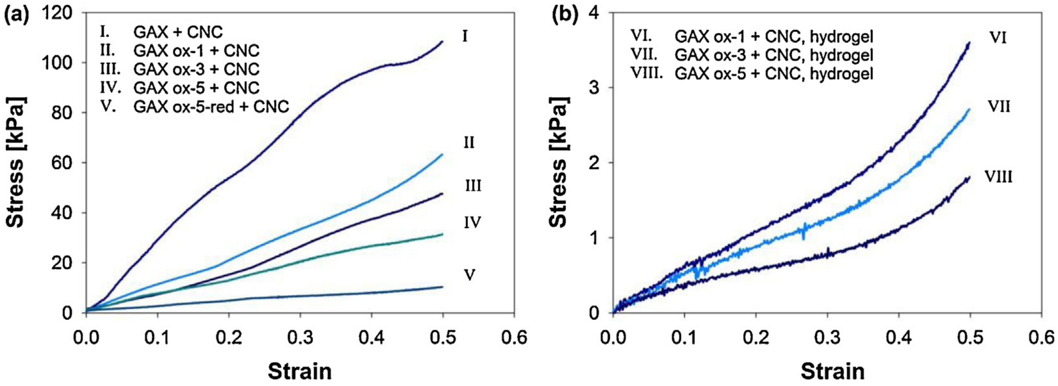

Fig. 7. Stress–strain curves of freeze-cast xylan–cellulose nanocrystal foams (a) and hydrogels (b).

Table 3
Stress-strain data of the different freeze-cast xylan-cellulose nanocrystal foams and hydrogels presented in this study.

Sample	Composition[a]	Stress at 50% strain [kPa]	Compressive modulus [kPa]
Dry			
I	GAX + CNC	109 ± 3	285 ± 76
II	GAX ox-1 + CNC	53 ± 9	86 ± 29
III	GAX ox-3 + CNC	47 ± 2	61 ± 19
IV	GAX ox-5 + CNC	33 ± 2	71 ± 22
V	GAX ox-5-red + CNC	12 ± 1	23 ± 7
Wet (25g H_2O/g)			
VI	GAX ox-1 + CNC	3.4 ± 0.4	5.4 ± 1.0
VII	GAX ox-3 + CNC	2.1 ± 0.6	3.8 ± 0.3
VIII	GAX ox-5 + CNC	1.9 ± 0.3	3.7 ± 0.7

[a] GAX = glucuronoarabinoxylan, CNCs = cellulose nanocrystals.

comparing data from the reference GAX material and the reduced oxidized GAX. Nevertheless, by comparing strength data from the oxidized sample and its reduced equivalent it is obvious that the cross-linking do have some strengthening effect. It should also be mentioned that even though there is a difference in compressive strength properties among the different samples, all samples formed free-standing biofoams.

The cross-linked biofoams were allowed to swell in water for 30 min and then tested for their compressive strength properties as hydrogels (Fig. 7b, Table 3). The strength properties decreased somewhat with the degree of oxidation. Again this probably has to do with the change in xylan molecular rigidity. Preparation of aldehyde xylan that does not involve opening of the xylan pyranose ring (cf. Chen et al., 2002) would probably solve this issue.

Finally something must be said about the stability of the formed hydrogels since hemiacetal linkages will hydrolyze in water. It was observed that the gelling effect slowly disappeared with time if the gels were kept immersed in water. After a couple of weeks the hydrogel was easily disintegrated by gentle shaking, and consequently the wet integrity of the obtained nanoreinforced xylan-based hydrogels must be considered to be temporary. Nevertheless, the wet integrity was preserved for a surprisingly long time even though individual hemiacetal linkages are unstable in water. This is probably due to the relatively high amounts of hemiacetal linkages in the system which will make the gels apparently resistant to water, and an increased degree of oxidation will consequently increase the stability of the gels in water over time.

4. Conclusions

This study shows that hemiacetal bonds are formed during freezing/freeze-drying of aldehyde xylans. The observation is used to obtain cross-linked xylan-based hydrogels from water suspensions by freeze-casting. If the xylan hydrogels are reinforced with 20% (w/w) CNCs, the ordered structure formed during the controlled freeze-casting process is maintained and free-standing hydrogels are formed with a water holding capacity of about 25 g H_2O/g material. The compressive strength properties of the dry freeze-cast foams decrease with increasing degree of xylan oxidation; probably due to changes in the rigidity of the xylan polymer chain upon oxidation, since oxidation involves opening of the xylan pyranose ring. In summary, this study describes a novel freeze-casting/cross-linking method which enables fabrication of nanoreinforced biopolymer-based hydrogels with tailor-made architectures.

Acknowledgements

The authors gratefully acknowledge financial support from the Gunnar Nicholson Foundation. Authors would also like to thank Angela Lin for training and use of equipment in the Biomechanics Core Facility at the Parker H. Petit Institute for Bioengineering and Bioscience at Georgia Institute of Technology, USA. Marcus Foston at Georgia Institute of Technology, USA, is acknowledged for assistance during NMR spectroscopy analyses.

References

Aliev, A. E., & Law, R. V. (2003). Solid-state NMR spectroscopy. *Nuclear Magnetic Resonance*, *32*, 238–292.
Brodin, F. W., & Theliander, H. (2012). Absorbent materials based on kraft pulp: Preparation and material characterization. *BioResources*, *7*, 1666–1683.
Chen, N., Hu, S., & Pelton, R. (2002). Mechanism of aldehyde-containing paper wet-strength resins. *Industrial & Engineering Chemistry Research*, *41*, 5366–5371.
Chimphango, A. F. A., van Zyl, W., & Görgens, J. F. (2012). *In situ* enzymatic aided formation of xylan hydrogels and encapsulation of horse radish peroxidase for slow release. *Carbohydrate Polymers*, *88*, 1109–1117.
Christensen, B. E., Aasprong, E., & Stokke, B. T. (2001). Gelation of periodate oxidised scleroglucan (scleraldehyde). *Carbohydrate Polymers*, *46*, 241–248.
Coviello, T., Matricardi, P., Marianecci, C., & Alhaique, F. (2007). Polysaccharide hydrogels for modified release formulations. *Journal of Controlled Release*, *119*, 5–24.

Deville, S. (2008). Freeze-casting of porous ceramics: A review of current achievements and issues. *Advanced Engineering Materials*, *10*, 155–169.

Duer, M. J. (2002). *Solid state NMR spectroscopy: Principles and applications*. Malden: Blackwell Science.

Ebringerová, A., & Heinze, T. (2000). Xylan and xylan derivatives – biopolymers with valuable properties, 1. *Macromolecular Rapid Communications*, *21*, 542–556.

Ebringerová, A., Hromáková, Z., & Heinze, T. (2005). Hemicellulose. In T. Heinze (Ed.), *Polysaccharides I. Advances in polymer science, 186* (pp. 1–67).

Eichhorn, S. J. (2011). Cellulose nanowhiskers: Promising materials for advanced applications. *Soft Matter*, *7*, 303–315.

Gutiérrez, M. C., Ferrer, M. L., & del Monte, F. (2008). Ice-templated materials: Sophisticated structures exhibiting enhanced functionalities obtained after unidirectional freezing and ice-segregation-induced self-assembly. *Chemistry of Materials*, *20*, 634–648.

Hansen, N. M. L., & Plackett, D. (2008). Sustainable films and coatings from hemicelluloses: A review. *Biomacromolecules*, *9*, 1493–1505.

Karaaslan, M. A., Tshabalala, M. A., Yelle, D. J., & Buschle-Diller, G. (2011). Nanoreinforced biocompatible hydrogels from wood hemicelluloses and cellulose whiskers. *Carbohydrate Polymers*, *86*, 192–201.

Kristiansen, K. A., Potthast, A., & Christensen, B. E. (2010). Periodate oxidation of polysaccharides for modification of chemical and physical properties. *Carbohydrate Research*, *345*, 1264–1271.

Köhnke, T., Brelid, H., & Westman, G. (2009). Adsorption of cationized barley husk xylan on kraft pulp fibres: Influence of degree of cationization on adsorption characteristics. *Cellulose*, *16*, 1109–1121.

Köhnke, T., Lin, A., Elder, T., Theliander, H., & Ragauskas, A. J. (2012). Nanoreinforced xylan–cellulose composite foams by freeze-casting. *Green Chemistry*, *14*, 1864–1869.

Köhnke, T., Lund, K., Brelid, H., & Westman, G. (2010). Kraft pulp hornification: A closer look at the preventive effect gained by glucuronoxylan adsorption. *Carbohydrate Polymers*, *81*, 226–233.

Köhnke, T., Östlund, Å., & Brelid, H. (2011). Adsorption of arabinoxylan on cellulosic surfaces: Influence of degree of substitution and substitution pattern on adsorption characteristics. *Biomacromolecules*, *12*, 2633–2641.

Köhnke, T., Theliander, H., & Ragauskas, A. J. (2012). Ice templated xylan-nanocrystalline cellulose aero/hydrogels. In *Book of Abstracts, 243rd ACS National Meeting, San Diego, CA, USA, March 25–29, CELL 171*.

Leary, G. J., Morgan, K. R., Newman, R. H., Samuelsson, B., & Westermark, U. (1986). A ^{13}C CP/MAS NMR comparison of wood fractions from spruce. *Holzforschung*, *40*, 221–224.

Lindblad, M. S., Sjöberg, J., Albertsson, A.-C., & Hartman, J. (2007). Hydrogels from polysaccharides for biomedical applications. In D. S. Argyropoulos (Ed.), *ACS symposium series Materials, chemicals, and energy from forest biomass* (pp. 153–167). American Chemical Society.

Maia, J., Carvalho, R. A., Coelho, J. F. J., Simões, P. N., & Gil, M. H. (2011). Imsight on the periodate oxidation of dextran and its structural vicissitudes. *Polymer*, *52*, 258–265.

Meena, R., Lehnen, R., Schmitt, U., & Saake, B. (2011). Effect of oat spelt and beech xylan on the gelling properties of *kappa*-carrageenan hydrogels. *Carbohydrate Polymers*, *85*, 529–540.

Newman, R. H., & Hemmingson, J. A. (1990). Determination of the degree of cellulose crystallinity in wood by carbon-13 nuclear magnetic resonance spectroscopy. *Holzforschung*, *44*, 351–355.

Painter, T., & Larsen, B. (1970). Transient hemiacetal structures formed during the periodate oxidation of xylan. *Acta Chemica Scandinavica*, *24*, 2366–2378.

Park, S., Johnson, D. K., Ishizawa, C. I., Parilla, P. A., & Davis, M. F. (2009). Measuring the crystallinity index of cellulose by solid state ^{13}C nuclear magnetic resonance. *Cellulose*, *16*, 641–647.

Peng, X.-W., Ren, J.-L., Zhong, L.-X., Peng, F., & Sun, R.-C. (2011). Xylan-rich hemicelluloses-*graft*-acrylic acid ionic hydrogels with rapid responses to pH, salt, and organic solvents. *Journal of Agricultural and Food Chemistry*, *59*, 8208–8215.

Peppas, N. A., Bures, P., Leobandung, W., & Ichikawa, H. (2000). Hydrogels in pharmaceutical formulations. *European Journal of Pharmaceutics and Biopharmaceutics*, *50*, 27–46.

Peppas, N. A., Hilt, J. Z., Khademhosseini, A., & Langer, R. (2006). Hydrogels in biology and medicine: From molecular principles to bionanotechnology. *Advanced Materials*, *18*, 1345–1360.

Pohjanlehto, H., Setälä, H., Kammiovirta, K., & Harlin, A. (2011). The use of *N,N′*-diallylaldardiamides as cross-linkers in xylan derivatives-based hydrogels. *Carbohydrate Research*, *346*, 2736–2745.

Ragauskas, A. J., Williams, C. K., Davison, B. H., Britovsek, G., Cairney, J., Eckert, C. A., et al. (2006). The path forward for biofuels and biomaterials. *Science*, *311*, 484–489.

Saito, T., & Isogai, A. (2006). Introduction of aldehyde groups on surfaces of native cellulose fibres by TEMPO-mediated oxidation. *Colloids and Surfaces A*, *289*, 219–225.

Saxena, A., & Ragauskas, A. J. (2009). Water transmission barrier properties of biodegradable films based on cellulosic whiskers and xylan. *Carbohydrate Polymers*, *78*, 357–360.

Schaefer, J., & Stejskal, E. O. (1976). Carbon-13 nuclear magnetic resonance of polymers spinning at the magic angle. *Journal of the American Chemical Society*, *98*, 1031–1032.

Silva, T. C. F., Habibi, Y., Colodette, J. L., & Lucia, L. A. (2011). The influence of the chemical and structural features of xylan on the physical properties of its derived hydrogels. *Soft Matter*, *7*, 1090–1099.

Van Vlierberghe, S., Dubruel, P., & Schacht, E. (2011). Biopolymer-based hydrogels as scaffolds for tissue engineering applications: A review. *Biomacromolecules*, *12*, 1387–1408.

Wegst, U. G. K., Schecter, M., Donius, A. E., & Hunger, P. M. (2010). Biomaterials by freeze casting. *Philosophical Transactions of the Royal Society A*, *368*, 2099–2121.

Zhao, H., & Heindel, N. D. (1991). Determination of degree of substitution of formyl groups in polyaldehyde dextran by the hydroxylamine hydrochloride method. *Pharmaceutical Research*, *8*, 400–402.